Brief Report

In Situ Biochemical Demonstration that P-Glycoprotein Is a Drug Efflux Pump with Broad Specificity

Yu Chen and Sanford M. Simon

Laboratory of Cellular Biophysics, Rockefeller University, New York 10021

Abstract. While P-glycoprotein (Pgp) is the most studied protein involved in resistance to anti-cancer drugs, its mechanism of action is still under debate. Studies of Pgp have used cell lines selected with chemotherapeutics which may have developed many mechanisms of resistance. To eliminate the confounding effects of drug selection on understanding the action of Pgp, we studied cells transiently transfected with a Pgp-green fluorescent protein (GFP) fusion protein. This method generated a mixed population of unselected cells with a wide range of Pgp-GFP expression levels and allowed simultaneous measurements of Pgp level and drug accumulation in living cells. The results showed that Pgp-GFP expression was inversely related to the accumulation of chemotherapeutic drugs. The reduction in

drug concentration was reversed by agents that block multiple drug resistance (MDR) and by the UIC2 anti-Pgp antibody. Quantitative analysis revealed an inverse linear relationship between the fluorescence of Pgp-GFP and MDR dyes. This suggests that Pgp levels alone limit drug accumulation by active efflux; cooperativity between enzyme, substrate, or inhibitor molecules is not required. Additionally, Pgp-GFP expression did not change cellular pH. Our study demonstrates the value of using GFP fusion proteins for quantitative biochemistry in living cells.

Key words: multiple drug resistance • green fluorescent protein • ATP cassette-binding proteins • chemotherapy • membrane transport

Introduction

Multidrug resistance (MDR)[1] is the major obstacle to the successful chemotherapeutic treatment of human cancers (Simon and Schindler, 1994; Ling, 1997). Often a cancer becomes resistant to many drugs of diverse structures and mechanisms after exposure to only a few drugs (Biedler et al., 1975; Bech-Hansen et al., 1976); it is then said to have developed multidrug resistance. Such MDR cancers often overexpress P-glycoprotein (Pgp), an ATP-binding cassette (ABC) protein encoded by the *MDR1* gene (Kartner et al., 1983; for a review, see Gottesman and Pastan, 1993; Stein, 1997; Wadkins and Roepe, 1997; Eytan and Kuchel, 1999). These cells are characterized by the

decreased accumulation of many classes of drugs, commonly called MDR drugs. The accumulation of MDR drugs in these cells is enhanced by other compounds known as MDR reversers.

Most studies of MDR have used drug-resistant cells generated by selection with chemotherapeutic drugs. These drugs are highly mutagenic and tumor cells are genetically unstable. Thus this selection process leads to a host of changes in cellular physiology that may result in drug resistance. Among them: decreased susceptibility to apoptosis (Robinson et al., 1997), increased DNA repair and drug metabolism (Deffie et al., 1988); increased cellular pH (Thiebaut et al., 1990; Roepe et al., 1993; Simon et al., 1994); decreased lysosomal and endosomal pH (Schindler et al., 1996; Altan et al., 1998); decreased plasma membrane potential (Roepe et al., 1993); increased plasma membrane conductance to chloride (Gill et al., 1992) and ATP (Abraham et al., 1993); and increased rates of vesicle transport (Altan et al., 1999). Studying a subclone after selection in chemotherapeutics has made it difficult to determine the degree to which Pgp contributes to MDR in any

Address correspondence to Sanford M. Simon, Laboratory of Cellular Biophysics, Rockefeller University, Box 304, 1230 York Avenue, New York, NY 10021. Tel.: (212) 327-8030. Fax: (212) 217-7543. E-mail: simon @rockefeller.edu

[1]*Abbreviations used in this paper:* ABC, ATP-binding cassette; AM, acetoxymethyl; GFP, green fluorescent protein; Ho342, Hoechst 33342; MDR, multidrug resistance; Pgp, P-glycoprotein; TMRE, tetramethyl-rhodamine methyl ester.

particular drug-selected cell line. It has also complicated studying Pgp's underlying mechanism. The most accepted mechanism is that Pgp is an ATP-dependent drug efflux pump. Alternatively, it has been proposed that Pgp raises the cytosolic pH and lowers the plasma membrane potential, thereby decreasing the accumulation of weak bases and positively charged drugs into the cytosol (Hoffman et al., 1996).

To elucidate the mechanism of Pgp, we used a novel technique of in situ biochemistry. We transiently expressed a fusion protein between Pgp and green fluorescent protein (GFP) to produce a mixed population of cells with a broad range of expression levels. Fluorescence was used to quantify simultaneously the expression and the activity of Pgp in individual cells. This eliminates the confounding aspects of drug selection or even clonal expansion. Expression of Pgp in the absence of drug selection was shown to be sufficient to produce drug resistance to a spectrum of unrelated chemotherapeutic drugs. The resulting quantification of the relation between Pgp expression and activity is consistent with the concept of Pgp as an active efflux pump and not consistent with cooperativity between either Pgp, substrate or inhibitor molecules. Finally, our study demonstrates the advantages of using in situ assays for quantitative biochemistry.

Materials and Methods

Cell Culture

HeLa cells (ATCC CCL-2) were cultured as per ATCC recommendations. MCF-7/ADR cells were cultured as described (Altan et al., 1998).

Construction and Expression of Vector

All restriction enzymes and T4 DNA ligase were from New England Biolabs. pGEM3Zf(−)Xba-MDR1.1, a phagemid containing the human *MDR1* cDNA, was purchased from ATCC. To make the PgpGFP fusion vector, site-directed mutagenesis using the UNG-DUT method (Kunkel, 1985) was performed to eliminate the 3′ stop codon and introduce a SalI site. The Pgp open reading frame was excised using XbaI on the 5′ end and SalI on the 3′ end and inserted into pEGFP-N1 (Clontech) cut with the NheI and SalI. PgpCFP was subsequently constructed by replacing the EGFP with ECFP from pECFP (Clontech). Transfections used Fugene 6 reagent (Roche Molecular Biomedical).

Fluorescent Microscopy

Epifluorescence microscopy was done on an inverted IX-70 microscope (Olympus America). The image was collected using the Orca cooled CCD camera (Hamamatsu Photonics), an IMAQ-1424 digital image acquisition card and in-house software written in LabVIEW (National Instruments). Excitation was provided using a 150 Watt Xenon arc lamp (OptiQuip). Excitation and emission filters were selected using filter wheels (Ludl Electronic Products). All filters were from Chroma. The following excitation and emission filters were used for epi-fluorescent microscopy: CFP: $\lambda_{ex} = 400$–430 nm, $\lambda_{em} = 460$–500 nm; GFP, BCECF, calcein, SNAFL-1, and SNAFL calcein: $\lambda_{ex} = 480$–490 nm, $\lambda_{em} = 500$–550 nm; Hoechst 342 and FURA-2: $\lambda_{ex} = 340$–380 nm, $\lambda_{em} = 430$–470 nm; tetramethyl-rhodamine methyl ester, SNARF-1, and SNARF calcein: $\lambda_{ex} = 530$–560 nm, $\lambda_{em} = 570$–650 nm.

Confocal microscopy was done on an upright Axiplan 2 microscope with a LSM 510 confocal attachment (Carl Zeiss). Excitation was provided by an Argon/Krypton laser with lines at 488 and 568 nm and a Helium/Neon laser at 633 nm. The following laser lines and emission filters were used for confocal microscopy: GFP: $\lambda_{ex} = 488$ nm, $\lambda_{em} = 500$–530 nm; Texas Red, Cy3, and TMRE: $\lambda_{ex} = 568$ nm, $\lambda_{em} = 580$ nm; LP, Fura Red, and daunorubicin: $\lambda_{ex} = 488$ nm, $\lambda_{em} = 580$ nm LP.

Immunofluorescence

Cells were plated on 18-mm glass coverslips placed in 12-well dishes. For Pgp surface staining, live cells were incubated with 1.22 µg/ml 4E3 (DakoA) or 2 µg/ml UIC2 (Immunotech), washed, stained with Texas red–conjugated anti–mouse IgG antibody at 1:500 (Sigma), and fixed. For tubulin staining, cells were incubated for 30 min in the presence of indicated concentrations of vincristine (Calbiochem), colchicine (Calbiochem), or nocodazole (Sigma). Cells were then fixed, permeabilized, and labeled with 2 µg/ml Cy3-labeled anti-β-tubulin antibody, clone TUB 2.1 (Sigma).

Dual Labeling with Drugs and Dyes in Living Cells

All fluorescent dyes were from Molecular Probes. Daunorubicin was from Calbiochem. Prior to observation, cells were incubated with the indicated drug or dye for the indicated amount of time in Opti-MEM without phenol red and with 10 mM Hepes (Life Technologies) in a 5% CO_2, 37°C incubator.

Ratiometric pH Imaging

SNARF-1 is a ratiometric pH indicator that emits at 640 nm in the basic form and 580 nm in the acidic form. Cells were loaded with 1 µM SNARF-1 AM in Opti-MEM for 30 min and resuspended in dye-free Opti-MEM before imaging. Three images were acquired for each field: GFP and SNARF-1 acid: $\lambda_{ex} = 530$–560 nm, $\lambda_{em} = 570$–590 nm; and SNARF-1 base: $\lambda_{ex} = 530$–560 nm, $\lambda_{em} = 600$–660 nm. Calibration was done as previously described (Altan et al., 1998).

FACS® Analysis

Cells were dissociated using Cell Stripper (Cellgro), incubated for 30 min in Opti-MEM with 50 nM TMRE and analyzed using FACScan® and CellQuest software (Becton Dickinson). GFP and TMRE fluorescence were acquired using FL1 (515–545 nm) and FL2 (564–606 nm), respectively. To estimate the number of GFP from fluorescence, 6-µm SPHERO yellow calibration particles (PharMingen) were used. The number of GFP molecules per cell was estimated to be 1.5× the FITC equivalent fluorescence units (Tsien, 1998).

Results

Effect of P-Glycoprotein GFP Fusion Protein Expression on Drug Accumulation

How much of the decreased accumulation of drugs and fluorescent dyes can be attributed to Pgp expression alone? Our approach was to transiently transfect cells with a fusion of Pgp and green or cyan fluorescent protein. This produced a diverse population of cells, ranging from those that expressed large amounts of Pgp to those that failed to express the protein at all. The activity of Pgp was then quantified in individual cells that had been exposed to the same treatments, but differed substantially in their levels of Pgp. Two assays were used to examine the effects of the Pgp-fluorescent protein on chemotherapeutic drugs. First, we examined the cellular accumulation of structurally divergent MDR fluorescent dyes including those that are constitutively positively charged, weakly basic or uncharged. Second, we measured the cellular activity of microtubule-disrupting chemotherapeutics by their effect on microtubules. Thus the activity of Pgp was quantitatively studied as a function of its levels of expression in individual cells.

To assure that a correctly folded, full-length fusion protein was produced in the transfected cells, we used immunoblotting and immunofluorescence. The PgpGFP fusion protein was detected as an ∼200-kD band by either an anti-Pgp antibody (clone F4) or anti-GFP antibody. Wild-

type Pgp appeared as an ~170 kD band (data not shown). Immunofluorescence of three epitope-specific anti-Pgp antibodies (clones F4, 4E3, and UIC2) colocalized with GFP fluorescence (data not shown).

Weak Base Chemotherapeutic Drugs

Daunorubicin is a weak base with one protonatable nitrogen at physiological pK_a (Altan et al., 1998). Cells expressing PgpGFP accumulated dramatically less daunorubicin (Fig. 1 A). Note that in this field, there were three cells that did not express Pgp (left), one that expressed a high level of protein (bottom right), and one that produced a small amount (top right, asterisk). The level of Pgp expression was inversely correlated with daunorubicin accumulation. For example, the daunorubicin fluorescence was >100-fold lower in the cell that expressed a high level of Pgp compared with its Pgp negative neighbor. Similarly, the level of Pgp expression was inversely related to the cellular accumulation of mitoxantrone, a clinically important anthracenedione chemotherapeutic that is also a weak base but that is significantly different in structure from daunorubicin (data not shown). The MDR reversers verapamil (40 μM, Fig. 1 A) and cyclosporin A (10 μM, data not shown), completely reversed the effect of PgpGFP expression on accumulation of daunorubicin. The UIC2 anti-Pgp antibody, at 10 μg/ml, partially reversed the effect of PgpGFP expression (data not shown).

Positively Charged Dyes

We tested the effects of expressing PgpGFP on two MDR compounds that have constitutive positive charges, the DNA stain Hoechst 33342 (Ho342) and the mitochondrial dye tetramethylrhodamine methyl ester (TMRE). (TMRE is similar to the well known MDR dye rhodamine 123 whose fluorescence overlaps GFP.) In cells expressing PgpGFP the TMRE fluorescence was virtually undetectable and the Ho342 fluorescence was threefold lower (Fig. 1 B), consistent with previous reports on the specificity of Pgp (Lizard et al., 1995b). The accumulation of both Ho324 and TMRE in the cells expressing PgpGFP was increased by the MDR-reversers verapamil (40 μM) and cyclosporin A (10 μM; data not shown). Staining with both TMRE and Ho342 serves as a good control for cell fitness. In unhealthy cells, the loss of mitochondrial membrane potential limits accumulation of TMRE while the degradation of the membrane permits large amounts of Ho342 to enter (Sun et al., 1992; Lizard et al., 1995a).

Acetoxymethyl Esters

The effects of PgpGFP expression was tested on a number of uncharged acetoxymethyl (AM) esters implicated as MDR substrates. AM esters of many hydrophilic indicator dyes are used to facilitate cellular loading (Homolya et al., 1993). Within the cell, esterases cleave AM groups, trapping the dye inside the cell. Expression of PgpCFP or PgpGFP substantially reduced the cellular accumulation of several AM esters such as Fura Red (Fig. 1 C). Adding verapamil (40 μM) increased Fura Red accumulation in PgpGFP-expressing cells (data not shown). The effects of PgpGFP on reducing the accumulation of BCECF, calcein, and Fura-2 (Table I) correlate with the ability of each

AM ester dye to stimulate the ATPase activity of Pgp (Homolya et al., 1993).

Microtubule-disrupting Drugs

We used a functional assay to quantify the effect of PgpGFP expression on the cytosolic activity of chemotherapeutics. Certain chemotherapeutics, such as colchicine, vincristine and nocodazole, depolymerize microtubules. The state of a cell's microtubules after being treated with these drugs is a measurement of the cellular concentration of the drug. Thus, we examined the microtubules using immunofluorescence against β-tubulin after drug treatment.

Cells expressing PgpGFP maintained microtubules in 80 nM vincristine while nonexpressing cells in the same field did not (Fig. 2 B). Cells expressing high levels of PgpGFP had intact microtubules even in 2 μM vincristine (Fig. 2 A). Thus, expression of PgpGFP correlates with a >25-fold decrease in vincristine accumulation. Expression of PgpGFP also decreased the sensitivity of cells to colchicine, but had no effect on sensitivity to nocodazole (Table II).

Expression Activity Profile of PgpGFP

Various mechanisms have been proposed to account for the effects of Pgp on drug accumulation in the cell (Wadkins and Roepe, 1997; Stein, 1997; Eytan and Kuchel, 1999). Each has a different characteristic dependence of drug accumulation on Pgp expression level. We used FACS® to quantify PgpGFP expression and TMRE accumulation over a wide dynamic range. Approximately 50% of HeLa cells expressed PgpGFP and the expression level varied >100-fold (Fig. 3 A). In cells expressing the highest level of PgpGFP, the average TMRE accumulation was 100-fold less than in nonexpressing cells. A dot plot of TMRE fluorescence versus GFP fluorescence shows an inverse linear relationship on a logarithmic scale with a slope close to −1, and a linear fit of slope −1 is shown as the solid line (Fig. 3 B). Hence, it appears that expression of PgpGFP has an inverse linear relationship to TMRE accumulation. This relationship is consistent only with a model in which Pgp mediates active efflux itself, without cooperativity between either enzyme or substrate (see below).

For an idealized cell with a plasma membrane efflux pump, where a single substrates interacts with a single enzyme, the steady-state ratio of cellular drug concentration (D_{in}) to external concentration (D_{out}) follows the following equation: $D_{in}/D_{out} \approx 1/(1 + X)$, where $X = N \cdot C/(K_m \cdot P \cdot S)$ (see Appendix). Here, N is the number of pumps, C

Table I. The Effect of PgpGFP or PgpCFP Expression on Accumulation of AM Esters

Dye	Effects on fluorescence
BCECF AM (CFP)	3–10-fold
Calcein AM (CFP)	>10-fold
Fura-2 AM (GFP)	>10-fold
Fura Red AM (GFP)	>10-fold
SNAFL-1 diacetate (CFP)	>10-fold
SNAFL calcein AM (CFP)	>10-fold
SNARF-1 AM (GFP)	>10-fold
SNARF calcein AM (GFP)	>3-fold
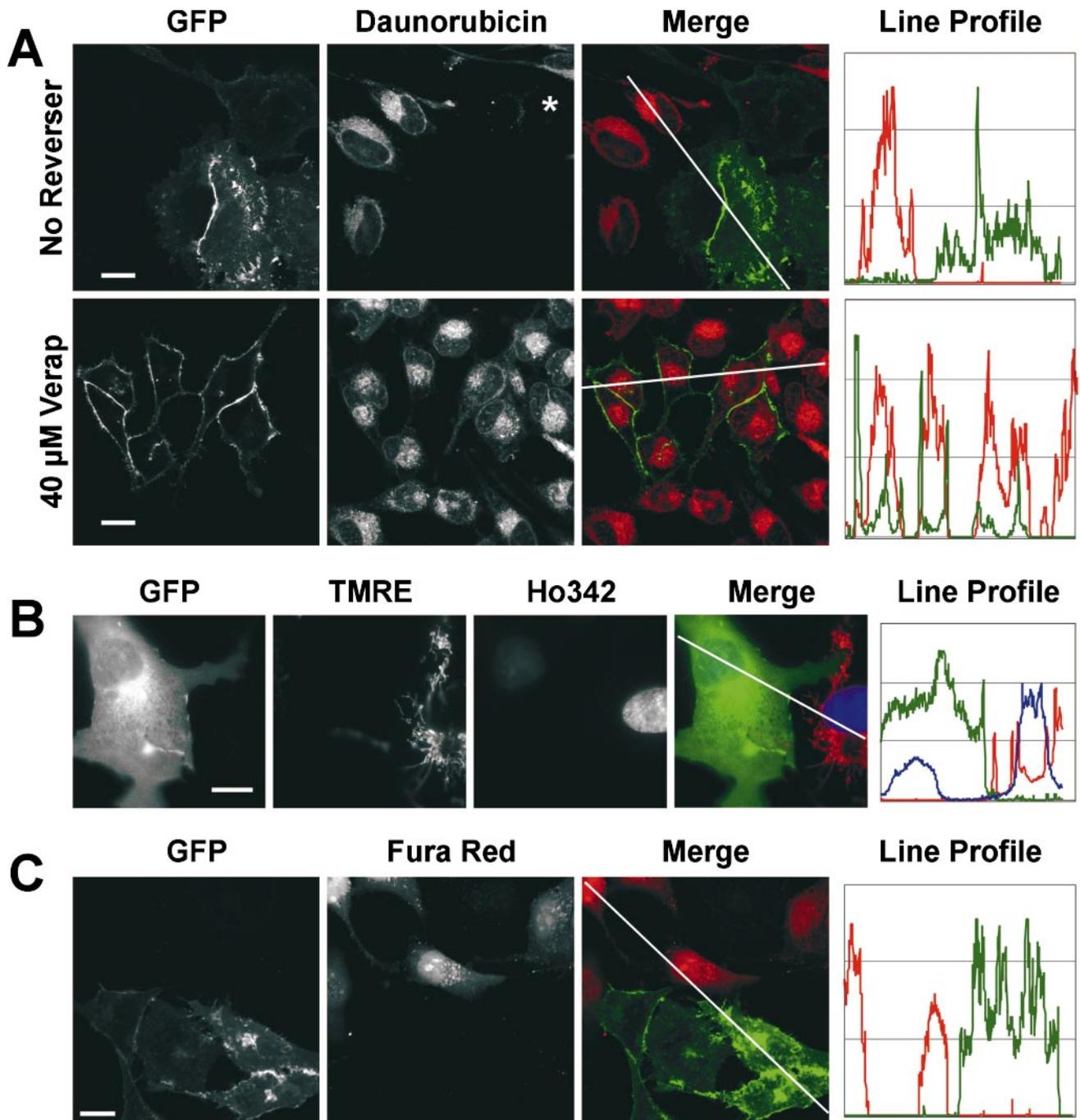
Figure 1. Effect of PgpGFP expression on the accumulation of fluorescent dyes. (A) PgpGFP-transfected HeLa cells were incubated for 30 min with 1 μM daunorubicin without (top) or with (bottom) 40 μg/ml verapamil. GFP and daunorubicin fluorescence were imaged using a confocal microscope. The fluorescence profile along the line drawn in the merge image was quantified (right). (B) Cells were incubated for 30 min with 200 nM TMRE and 200 nM Ho342, and the fluorescence images of GFP, TMRE, and Ho342 were acquired using an epifluorescence microscope. (C) Cells were incubated for 30 min with 5 μM Fura Red AM and GFP and Fura Red fluorescence were imaged on a confocal microscope. Bars, 20 μm.

is the catalytic constant, P is the drug permeability and S is the plasma membrane surface area. When X is <1, the cellular drug concentration approaches the external drug concentration and increasing X has little effect. When X is >1, the ratio approaches $1/X$, an inversely linear relationship. We modeled this equation using the following approximate constants: $P = 10^{-5}$ cm/s, $S = 5,000$ μm², $K_m = 10$

μM. Fig. 3 H shows a plot D_{in}/D_{out} as a function of the number of pump molecules per cell. The five plots, from left to right, assume catalytic constants of 10, 1, 0.1, 0.01, and 0.001 drug molecules pumped per Pgp per second.

The model predicts that an inhibitor should shift the TMRE accumulation to PgpGFP relationship to the right, analogous to decreasing the catalytic constant in Fig. 3 H.
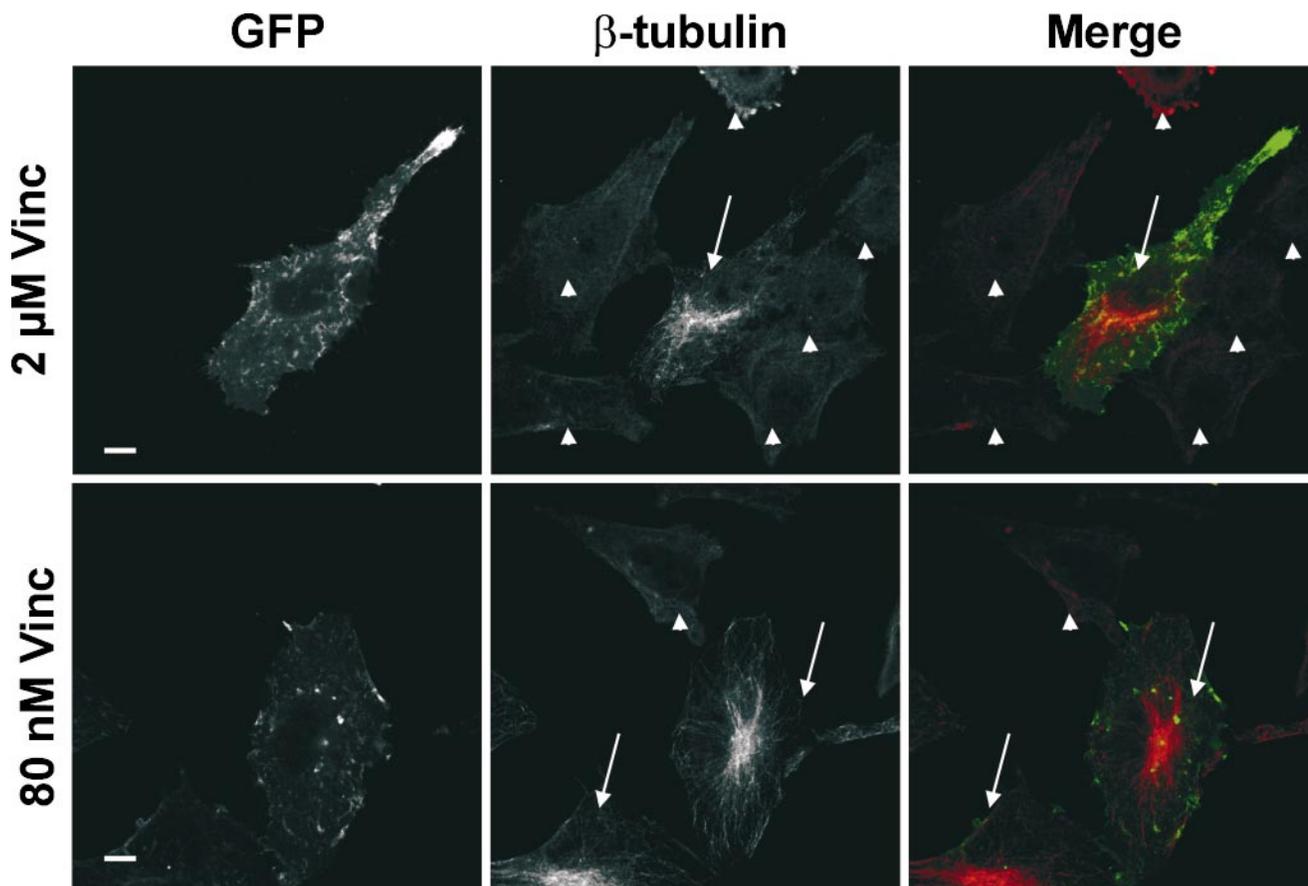
Figure 2. Effect of PgpGFP expression on vincristine-mediated microtubule depolymerization. PgpGFP-transfected HeLa cells were incubated with 2 µM or 80 nM vincristine for 30 min and stained with a Cy3-conjugated anti-β-tubulin antibody. Arrows indicate PgpGFP expressing cells and arrowheads indicate nonexpressing cells. Bars, 20 µm.

This was tested by coincubating cells with TMRE and 3.13, 6.25, 12.5, 25, or 50 µM verapamil (Figs. 3, C–G, respectively). The solid lines on these figures is the fit from Fig. 3 B as a reference. Indeed, as the concentration of verapamil increased, the curve shifted right. To quantify the effect of verapamil, we estimated the average TMRE fluorescence of cells showing GFP fluorescence of 10^3 at different verapamil concentrations using the dash lines in Figs. 3, B–G. The plot of TMRE fluorescence versus verapamil concentration shows an approximate linear relationship (Fig. 3 I), as expected from a specific inhibitor and lack of cooperativity between inhibitor molecules (see Appendix). Our data estimate the K_i of verapamil to be 3 µM, in full agreement with published data (Lan et al., 1996). Thus, the FACS® data shows that Pgp mediates active drug efflux, and that verapamil is a specific inhibitor.

Table II. The Effect of High Level PgpGFP Expression on Drug-mediated Microtubule Depolymerization

Drug	Fold resistance
Colchicine	5–25-fold
Nocodazole	None
Vincristine	25–125-fold

Effect of PgpGFP Expression on Cellular pH

MDR cells have been shown to have higher cytosolic pH (Keizer and Joenje, 1989; Simon et al., 1994). Since such higher pH results in decreased concentration of weak base drugs this could be the consequence of selection in chemotherapeutics rather than a specific effect of expressing Pgp. However, stable transfection of Pgp has been reported to raise cytosolic pH (Thiebaut et al., 1990) even without chemotherapeutic drug selection (Hoffman et al., 1996).

We examined the effect of PgpGFP expression on cytosolic pH using SNARF-1. Fig. 4, A–F, show calibration at three different pH. As expected, the ratio increased with increasing pH in an exponential manner. PgpGFP expression did not affect the ratio of the calibration images. Measurement of cellular pH of cells in medium showed that both PgpGFP expressing and nonexpressing cells had a cytosolic pH of ∼7.2 (Fig. 4, G and H). Thus, Pgp expression has no effect on cellular pH.

Discussion

The goal of our study was to determine if Pgp expression in the absence of any selection was sufficient to produce multidrug resistance and, if so, to understand the mechanism of Pgp. To this end, we devised a technique that al-

Figure 3. FACS® analysis of TMRE accumulation as a function of PgpGFP expression. (A) Histogram of GFP fluorescence of HeLa cells transfected with PgpGFP. Approximately 50% of the cells were nonexpressing showing a single peak of $\sim5 \times 10^0$ units. Transfected cells showed a >100-fold range of GFP fluorescence. (B) Dot plot of transfected cells incubated for 30 min with 50 nM TMRE. The solid diagonal line of slope -1 was fit to the data. To estimate the average TMRE fluorescence exhibited by cells with GFP fluorescence of 10^3 units, a dashed line was drawn from the center of cell density at 10^3 down and across to the x and y axes. At all levels of PgpGFP expression, there were some cells that showed TMRE fluorescence of 10^2 on the y-axis (marked as a horizontal oval). Coincubation with propidium iodide selectively increased the fluorescence of these cells, indicating that they were most likely dead (data not shown). (C–G) Dot plot of cells coincubated with the indicated verapamil concentration. The solid diagonal line was repro-

duced from B for reference. The average TMRE fluorescence exhibited by cells with GFP fluorescence of 10^3 units was estimated as in B. (H) The ratio of drug in/drug out was modeled is described in text. Plots of D_{in}/D_{out} as a function of number of Pgp per cell are shown for five different catalytic constants of 10, 1, 0.1, 0.01, and 0.001 drug molecules per pump per second. (I) Plot of average TMRE fluorescence of cells exhibiting GFP fluorescence of 10^3 as a function of verapamil concentration from the dash lines drawn in B–G. Open circle indicates no verapamil control (not 1 μm).

lowed the levels of Pgp expression to be directly compared with cellular accumulation of chemotherapeutics. We designed a novel method that took advantage of GFP, a protein that has revolutionized cell biology by permitting the study of localization and movement of proteins in living cells. We extended the range of application of GFP to the study of biochemical processes in living cells. Traditionally, enzymes are studied in vitro, away from their natural cellular environment. Enzyme analysis in living cells is hampered by two constraints. First, intracellular enzyme concentration usually varies within a narrow range, and second, enzyme concentration and intracellular localization cannot be easily measured. The use of transient transfection addresses the first problem since it generates a large range of expression levels. Using GFP fusion proteins addresses the second problem. A previous approach to in vivo enzyme analysis also employed transient transfection of the enzyme. In that study, enzyme activity was detected with a fluorescent substrate. The amount of enzyme was measured by subsequent immunoquantification

(Morita et al., 1995). Using a GFP fusion protein allowed us to measure simultaneously the quantity, localization and kinetic activity of an enzyme in living cells.

Expression of PgpGFP resulted in dramatically decreased accumulation of many diverse compounds, including the noncharged AM-esters, the weak base drug daunorubicin, and the constitutively charged dyes TMRE and Ho342. Decreased accumulation was also inferred from the decreased sensitivities to microtubule depolymerizing drugs vincristine and colchicine. This effect of PgpGFP expression was inhibited by an antibody against Pgp and MDR reversers.

FACS® analysis showed that PgpGFP expression and TMRE accumulation had an inverse linear relationship, implying that PgpGFP mediates active efflux. Furthermore, this data implies that the TMRE extrusion is a bimolecular reaction: a single molecule of TMRE is pumped at a time and a single Pgp unit (monomer or stable multimer) is the catalytic unit. FACS® analysis further showed that the concentration of verapamil and level of TMRE

868

Figure 4. Effect of PgpGFP expression on cellular pH. PgpGFP-transfected HeLa cells were loaded with SNARF-1 by a 30-min incubation with 1 μM SNARF-1 AM. (A–F) SNARF-1 was calibrated by measuring the fluorescence cells incubated in calibration solution at pH 6.75, 7.25, and 7.75 (shown), and 7.0, 7.5, and 8.0 (not shown). The GFP image identifies PgpGFP expressing cells (left). The ratio of the SNARF-1 base/acid fluorescence are shown as a pseudocolor intensity image (right). The scale on the right of the lookup color bar represents the average SNARF-1 ratio calibrated at the indicated pH values. (G–H) The GFP and SNARF-1 fluorescent ratio images of cells in media. Bar, 20 μM.

accumulation in PgpGFP expressing cells were linearly related, suggesting that verapamil is an inhibitor and that there is no interaction between pairs of verapamil molecules.

Tumor cells are known to be genetically unstable and that exposure to mutagenic compounds invariably results in many mechanisms of drug resistance. Which combinations of these mechanisms are clinically relevant has yet to be established. The use of GFP fusions permits the study of any one individual protein independently from other drug resistance phenomena.

Appendix

We use the pump/leak model (Stein, 1997; Eytan and Kuchel, 1999). The drug influx rate is the leak in and the drug efflux rate is the leak out plus the pump rate out:

$$Influx = P \cdot S \cdot D_{out} \text{ and}$$

$$Efflux = P \cdot S \cdot D_{in} + N \cdot C \cdot D_{in}/(D_{in} + K_m),$$

where the constants are defined in the text. To further simplify our analysis, we assume that D_{in} is small compared with K_m, which is safe since we used a TMRE concentra-

tion of 50 nM. The pump rate then approximates $N \cdot C \cdot D_{in}/K_m$. The equilibrium concentration must satisfy the equation $Influx = Efflux$, giving

$$D_{in}/D_{out} \approx 1/(1 + X); X = N \cdot C/(K_m \cdot P \cdot S).$$

A noncompetitive inhibitor decreases the apparent C according to the following formula:

$$C_{app}/C = (K_i/K_i + I),$$

where I is the inhibitor concentration. Thus, the apparent C is halved when $I = K_i$. When $I >> K_i$, C_{app} approaches an inverse linear relationship with I. For a competitive inhibitor, the apparent K_m is increased such that

$$K_m/K_{mapp} = K_i/K_i + I,$$

and the same analysis shows that when $I = K_i$, K_{mapp} is doubled and K_{mapp} is linearly related to I when $I >> K_i$.

References

Abraham, E.H., A.G. Prat, L. Gerweck, T. Seneveratne, R.J. Arceci, R. Kramer, and G. Guidotti. 1993. The multidrug resistance (*mdr1*) gene product functions as an ATP channel. *Proc. Natl. Acad. Sci. USA.* 90:312–316.

Altan, N., Y. Chen, M. Schindler, and S.M. Simon. 1998. Defective acidification in human breast tumor cells and implications for chemotherapy. *J. Exp. Med.* 187:1583–1598.

Altan, N., Y. Chen, M. Schindler, and S.M. Simon. 1999. Tamoxifen inhibits acidification in cells independent of the estrogen receptor. *Proc. Natl. Acad. Sci. USA.* 96:4432–4437.

Bech-Hansen, N.T., J.E. Till, and V. Ling. 1976. Pleiotropic phenotype of colchicine-resistant CHO cells: cross-resistance and collateral sensitivity. *J. Cell. Physiol.* 88:23–31.

Biedler, J.L., H. Riehm, R.H. Peterson, and B.A. Spengler. 1975. Membrane-mediated drug resistance and phenotypic reversion to normal growth behavior of Chinese hamster cells. *J. Natl. Canc. Inst.* 55:671–680.

Deffie, A.M., T. Alam, C. Seneviratne, S.W. Beenken, J.K. Batra, T.C. Shea, W.D. Henner, and G.J. Goldenberg. 1988. Multifactorial resistance to adriamycin: relationship of DNA repair, glutathione transferase activity, drug efflux, and P-glycoprotein in cloned cell lines of adriamycin-sensitive and -resistant P388 leukemia. *Cancer Res.* 48:3595–3602.

Eytan, G.D., and P.W. Kuchel. 1999. Mechanism of action of P-glycoprotein in relation to passive membrane permeation. *Int. Rev. Cytol.* 190:175–250.

Gill, D.R., S.C. Hyde, C.F. Higgins, M.A. Valverde, G.M. Mintenig, and F.V. Sepúlveda. 1992. Separation of drug transport and chloride channel functions of the human multidrug resistance P-glycoprotein. *Cell.* 71:23–32.

Gottesman, M.M., and I. Pastan. 1993. Biochemistry of multidrug resistance mediated by the multidrug transporter. *Annu. Rev. Biochem.* 62:385–427.

Hoffman, M.M., L.Y. Wei, and P.D. Roepe. 1996. Are altered pHi and membrane potential in hu MDR 1 transfectants sufficient to cause MDR protein-mediated multidrug resistance? *J. Gen. Physiol.* 108:295–313.

Homolya, L., Z. Holló, U.A. Germann, I. Pastan, M.M. Gottesman, and B. Sarkadi. 1993. Fluorescent cellular indicators are extruded by the multidrug resistance protein. *J. Biol. Chem.* 268:21493–21496.

Kartner, N., J.R. Riordan, and V. Ling. 1983. Cell surface P-glycoprotein associated with multidrug resistance in mammalian cell lines. *Science.* 221:1285–1288.

Keizer, H.G., and H. Joenje. 1989. Increased cytosolic pH in multidrug-resistant human tumor cells: effect of verapamil. *J. Natl. Cancer Inst.* 81:706–709.

Kunkel, T.A. 1985. Rapid and efficient site-specific mutagenesis without phenotypic selection. *Proc. Natl. Acad. Sci. USA.* 82:488–492.

Lan, L.B., S. Ayesh, E. Lyubimov, I. Pashinsky, and W.D. Stein. 1996. Kinetic parameters for reversal of the multidrug pump as measured for drug accu-

mulation and cell killing. *Cancer Chemother. Pharmacol.* 38:181–190.

Ling, V. 1997. Multidrug resistance: molecular mechanisms and clinical relevance. *Cancer Chemother. Pharmacol.* 40:S3–S8.

Lizard, G., S. Fournel, L. Genestier, N. Dhedin, C. Chaput, M. Flacher, M. Mutin, G. Panaye, and J.P. Revillard. 1995a. Kinetics of plasma membrane and mitochondrial alterations in cells undergoing apoptosis. *Cytometry.* 21:275–283.

Lizard, G., M. Maynadie, P. Roignot, S. Lizard-Nacol, and M.F. Poupon. 1995b. Evaluation of multidrug resistant phenotype by flow cytometry with monoclonal antibodies and functional tests. *Bull. Cancer.* 82:211–217.

Morita, I., W.L. Smith, D.L. DeWitt, and M. Schindler. 1995. Expression-activity profiles of cells transfected with prostaglandin endoperoxide H synthase measured by quantitative fluorescence microscopy. *Biochemistry.* 34:7194–7199.

Robinson, L.J., W.K. Roberts, T.T. Ling, D. Lamming, S.S. Sternberg, and P.D. Roepe. 1997. Human MDR 1 protein overexpression delays the apoptotic cascade in Chinese hamster ovary fibroblasts. *Biochemistry.* 36:11169–11178.

Roepe, P.D., L. Yong Wei, J. Cruz, and D. Carlson. 1993. Lower electrical membrane potential and altered pH_i homeostasis in multidrug-resistant (MDR) cells: further characterization of a series of MDR cell lines expressing different levels of P-glycoprotein. *Biochemistry.* 32:11042–11056.

Schindler, M., S. Grabski, E. Hoff, and S.M. Simon. 1996. Defective pH regulation of acidic compartments in human breast cancer cells (MCF-7) is normalized in adriamycin-resistant cells (MCF-7adr). *Biochemistry.* 35:2811–2817.

Simon, S.M., and M. Schindler. 1994. Cell biological mechanisms of multidrug resistance in tumors. *Proc. Natl. Acad. Sci. USA.* 91:3497–3504.

Simon, S.M., D. Roy, and M. Schindler. 1994. Intracellular pH and the control of multidrug resistance. *Proc. Natl. Acad. Sci. USA.* 91:1128–1132.

Stein, W.D. 1997. Kinetics of the multidrug transporter (P-glycoprotein) and its reversal. *Physiol. Rev.* 77:545–590.

Sun, X.M., R.T. Snowden, D.N. Skilleter, D. Dinsdale, M.G. Ormerod, and G.M. Cohen. 1992. A flow-cytometric method for the separation and quantitation of normal and apoptotic thymocytes. *Anal. Biochem.* 204:351–356.

Thiebaut, F., S.J. Currier, J. Whitaker, R.P. Haugland, M.M. Gottesman, I. Pastan, and M.C. Willingham. 1990. Activity of the multidrug transporter results in alkalinization of the cytosol: measurement of cytosolic pH by microinjection of a pH-sensitive dye. *J. Histochem. Cytochem.* 38:685–690.

Tsien, R.Y. 1998. The green fluorescent protein. *Annu. Rev. Biochem.* 67:509–544.

Wadkins, R.M., and P.D. Roepe. 1997. Biophysical aspects of P-glycoprotein-mediated multidrug resistance. *Intl. Rev. Cytol.* 171:121–165.